

Photoelectrochemical Behaviour of Pulse Plated $\text{CuIn}_{0.6}\text{Al}_{0.4}\text{Se}_2$ Thin Films

M.Thirumoorthy, K.Ramesh, K.R.Murali

Abstract— $\text{CuIn}_{0.6}\text{Al}_{0.4}\text{Se}_2$ films were pulse electrodeposited on tin oxide coated glass substrates at different duty cycles for the first time. The films were single phase with chalcopyrite structure. The crystallite size of the films increased from 15 nm – 40 nm. Optical absorption measurements indicated a band gap in the range of 1.97 eV to 2.07 eV with increase of duty cycle. Transmission spectra exhibited interference fringes. Using the envelope method, refractive index value was calculated. The refractive index increased with increase of duty cycle. Photoelectrochemical cells were fabricated using the films deposited at different duty cycle. Polysulphide redox electrolyte was used for the studies. In order to induce photoactivity the films were post heat treated in argon atmosphere at different temperatures in the range of 450°C - 525°C. The films post heat treated at 500°C exhibited maximum photooutput. The films were photoetched in dilute HNO_3 . The photooutput was V_{oc} of 0.59V, J_{sc} of 13.7 mA cm^{-2} , ff of 0.65 and efficiency of 8.75 % at 60 mW cm^{-2} illumination from tungsten halogen lamp after photoetching.

Index Terms—Thin films, electronic material, semiconductor, I-III-VI₂ semiconductor, chalcopyrite structure, Photoelectrochemical (PEC) cells, Photovoltaics

1 INTRODUCTION

THE chalcopyrite CuInSe_2 (CIS) is a very interesting material used as absorber layer in thin film solar cells. In order to increase the CIS band gap for an optimal match with solar radiation spectrum and to improve thereby the module performance, CIS is usually alloyed with Ga or S. With Cu(In,Ga)Se_2 absorber layers cell efficiencies around 19.5% have been achieved on laboratory scale [1]. However, Ga is a rare and costly material that can be replaced by low-cost and abundant Al. For this reason, Cu(In,Al)Se_2 (CIAS) has been considered as promising alternative, since it requires less aluminium concentration than gallium to achieve a similar band gap [2]. Cu(In, Al)Se_2 thin films have been prepared by several techniques including co-evaporation [3,4], chemical bath deposition (CBD) [5], one step RF magnetron sputtering [6] and sequential deposition methods [7]. The co-evaporation technique gives the highest efficiency of Cu(In,Al)Se_2 based solar cells with 16.9% [3] but presents difficulties in upscaling. In this work, the pulse electrodeposition technique was employed for the first time to deposit CIAS thin films and the results are presented.

2 Experimental Methods

In comparison to DC electrodeposition, pulsed current (PC) electrodeposition is known to offer several advantages

since it provides additional variables such as duty cycle and amplitude of pulsed current/potential. The duty cycle is defined as follows:

$$\text{Duty Cycle (\%)} = (\text{ON time}) / (\text{ON time} + \text{OFF time}) \times 100 \quad (1)$$

Appropriate regulation of these variables can be used for suitable manipulation of diffusion layer, grain size and nucleation. This, in turn, results in better deposit homogeneity as well as exact control over stoichiometry and deposition rate. During the deposition of thin films of ternary/quaternary systems, such control over the composition of individual elements is particularly crucial to obtain single-phase by controlling the formation of secondary phases, thereby making PC electrodeposition an attractive technique [8], [9]. Furthermore, by varying the duty cycle, reduction in porosity can be achieved by avoiding entrapment of hydrogen during deposition and results in a highly dense and compact films [10], [11]. In general, electrodeposition of Al and In is relatively difficult due to their more negative reduction potentials compared to Cu and Se. It has also been observed earlier, for copper indium gallium selenide (CIGS), that the In content decreases with increase in pulse off-time (low duty cycles), during the PC electrodeposition of CIGS thin-films [8], [9]. Due to these reasons, high concentration of Al and In precursor have been used to adjust the In and Al content in the films, in order to obtain stoichiometric CIAS thin films

CIAS thin films were deposited by the pulse plating technique using non aqueous ethylene glycol solution. 0.2 M $\text{Al}_2(\text{SO}_4)_3$, 0.1 M $\text{In}_2(\text{SO}_4)_3$, 0.02 M CuSO_4 , 0.05 M SeO_2 . The films were deposited at 80°C and at different duty cycles at a constant current density of 5 mA cm^{-2} . Tin oxide coated glass (5 ohms/sq) were used as substrates. Conventional aqueous solutions cannot be always used as electrolytes due to the liberation of hydrogen molecule during electrolysis, narrow electrochemical windows, low thermal stability, and evaporation. These are the reasons why scientists have searched for non-

- M.Thirumoorthy, Department of Physics, Shree Venkateshwara Hi-Tech Engineering College, Gobi 638455, India, PH-9944710686. E-mail: thirumoorthyvhec@gmail.com
- K.Ramesh, Department of Physics, Government Art College, C-Mutlur, Chidambaram, India
- K.R.Murali, Department of Theoretical Physics, University of Madras, India

aqueous solutions to electrodeposit thin films. Thickness of the films measured using Mitutoyo surface profilometer was in the range of 600 nm – 1100 nm with increase of duty cycle from 6 – 50 %. The films were characterized by Xpert analytical x-ray diffraction unit with CuK α radiation. Composition of the films was estimated by EDS attachment to JOEL SEM. Optical measurements were made at room temperature with Hitachi U3400 UV-VIS-NIR spectrophotometer. Photoelectrochemical cell measurements were made with 1 M polysulphide (1 M S, 1 M Na₂S, 1 M NaOH) as the redox electrolyte with 250 W tungsten halogen lamp as the light source.

3 RESULTS AND DISCUSSION

The X-ray diffraction pattern of CIAS films formed at different duty cycles is shown in Fig.1. The films were polycrystalline exhibiting the peaks corresponding to the single phase CIAS. Peaks corresponding to (112), (220), (204), (312) and (116) orientations of the chalcopyrite structure were observed, similar to earlier reports [12]. The evaluated lattice parameters were around $a = 5.62 \text{ \AA}$ and $c = 10.99 \text{ \AA}$. The crystallite size was calculated from the Full width half maximum of the diffraction profiles using Scherrer's equation

$$D = 0.95 \lambda / (\beta \cos \theta) \quad (2)$$

Where, D is the crystallite size, λ is the wavelength of CuK α radiation, β is the full width at half maximum, θ is the Bragg angle. The crystallite size increased from 15 nm – 40 nm as the duty cycle decreased from 50 % - 6 %. The crystallite size and thickness of the films are shown in Table.1.

The dislocation density δ , defined as the length of dislocation lines per unit volume of the crystal has been evaluated using the formula [13]

$$\delta = 1/D^2 \quad (3)$$

The dislocation density is also presented in Table-1. From the table it is observed that the dislocation density decreases with increase of grain size. Information on the particle size and strain for the CIAS films was obtained from the full-width at half-maximum of the diffraction peaks. The full-width at half-maximum β can be expressed as a linear combination of the contributions from the particle size, D and strain, ϵ through the relation

$$\beta \cos \theta / \lambda = 1/D + \epsilon \sin \theta / \lambda \quad (4)$$

The plot of $\beta \cos \theta / \lambda$ vs $\sin \theta / \lambda$ allows us to determine both strain and particles size from slope and intercept of the graph. The estimated values of strain for films deposited at different duty cycles are also listed in Table - 1. The difference in the lattice parameter values from the bulk value experimental in the current case evidently suggest that the grains in the films are in stress. Such behaviour can be accredited to the change of nature, deposition conditions and the concentration of the native imperfections developed in thin films. This results in either elongation or compression of the lattice and the structural parameters. The density of the film is therefore found to change considerably in accordance with the variations observed with the lattice constant values. The defects have a probability to migrate parallel to the substrate surface so that the films will have a tendency to expand and develop an in-

ternal tensile stress. This type of change in internal stress is always predominant by the observed recrystallization process in polycrystalline films. The stress relaxation is mainly considered as due to dislocation glides formed in the films. The decrease of internal stress may be attributed to a decrease in dislocation density. The decrease in the strain and dislocation density with increase of duty cycle may be due to the decrease in concentration of lattice imperfections at superior duty cycle.

Composition of the films was determined by the Energy dispersive x-ray analysis (EDAX) attachment of the Scanning Electron Microscope (SEM). Decreasing the duty cycle from 50% to 15% reduces the relative content of Al and Se, but has no obvious effect on Indium relative content in the film, this can be attributed to the fact that Al was first dissolved back into the solution due to its lowest electronegativity corresponding to the positive current during the non pulse duration t_{off} , leading to the loss of Al in the deposited film, and therefore reduction of Al-Se compound(s). Similar phenomenon also has been observed during the pulse electrodeposition of ternary CuInSe₂ [14]. When duty cycle further decreases to 6 %, besides significant loss of Al, the relative content of indium also indicates some drop, thereby leading to a corresponding reduction of In-Se compound(s). Due to the above mentioned reasons, the composition of the films deposited at 50 % duty cycle was CuIn_{0.6}Al_{0.4}Se₂, which decreased to CuIn_{0.6}Al_{0.38} at 33 % duty cycle, and to CuIn_{0.58}Al_{0.36}Se₂, CuIn_{0.56}Al_{0.34}Se₂, CuIn_{0.55}Al_{0.33}Se₂ for 15 %, 9 % and 6 % duty cycle respectively.

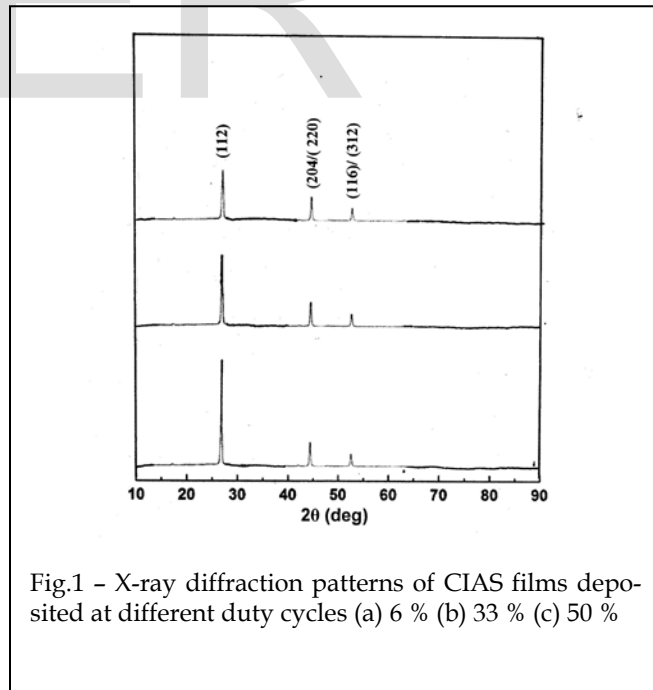


Fig.1 - X-ray diffraction patterns of CIAS films deposited at different duty cycles (a) 6 % (b) 33 % (c) 50 %

Fig.2 shows the transmission spectra of the CIAS films deposited at different duty cycles. The spectra exhibit interference fringes and the value of the refractive index was estimated by the envelope method [15] as follows:

Table.1
Structural parameters of CuIn_{0.6}Al_{0.4}Se₂ films deposited at different duty cycles.

Duty cycle (%)	Thickness (nm)	Crystallite size (nm)	Internal stress (Gpa)	Dislocation density (10 ¹⁵ lines m ⁻¹)
6	600	40	-0.22	4.4
9	720	32	-0.15	2.9
15	840	26	-0.12	1.8
33	970	21	-0.05	0.7
50	1100	15	-0.01	0.2

$$n = [N + (N^2 - n_s^2)^2] \quad (3)$$

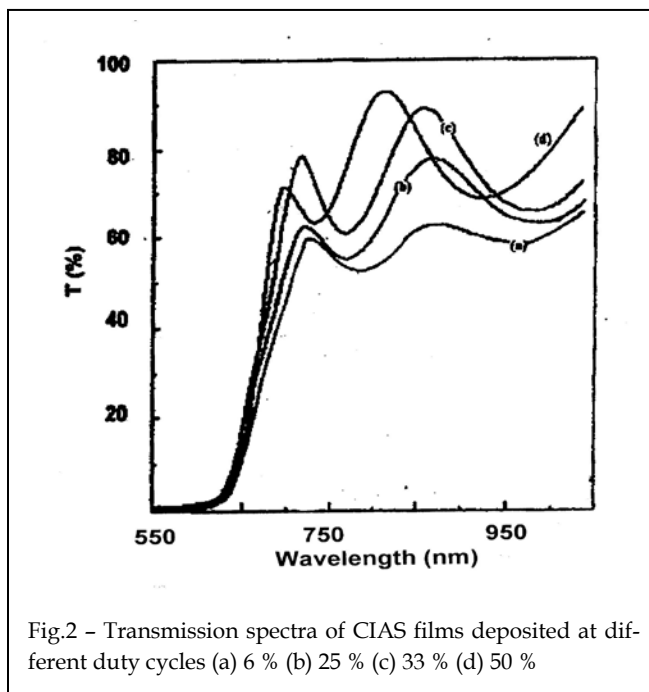
$$N = (n_s^2 + 1)/2 + 2 n_s (T_{max} - T_{min}) / T_{max} T_{min} \quad (4)$$

where n_s is the refractive index of the substrate, T_{max} and T_{min} are the maximum and minimum transmittances at the same wavelength in the fitted envelope curve on a transmittance spectrum. The value of the refractive index at 350 nm, calculated from the above equations was in the range of 2.90 - 2.70 for the samples deposited at different duty cycle. The value of the absorption co-efficient (α) was calculated using the relation

$$\alpha = 1/d \ln \left\{ \frac{(n-1)(n-n_s)}{(n+1)(n-n_s)} \right\} \left[\frac{(T_{max}/T_{min})^2 + 1}{(T_{max}/T_{min})^2 - 1} \right] \quad (5)$$

where 'd' is the thickness of the film and the other parameters have the usual meaning as given for equation (4). The films exhibited a high absorption co-efficient of the order of 10⁴ cm⁻¹. A plot of $(ahv)^2$ against hv , as indicated in Fig. 3, exhibits linear behavior near the band edge, the band gap of the deposited films was determined to be in the range of 1.97 - 2.01 eV. This value agrees well with earlier report on thermally evaporated CuIn_{0.6}Al_{0.4}Se₂ films [16].

Photoelectrochemical (PEC) cells were prepared using the films deposited at 80°C and at different duty cycles. The films were lacquered with polystyrene in order to prevent the metal substrate portions from being exposed to the redox electrolyte. These films were used as the working electrode. Photoelectrochemical cell studies were made using 1.0 M Na₂S, 1.0 M NaOH and 1.0 M S, as the redox electrolyte. Graphite was used as the counter electrode. The light source used for illumination was an ORIEL 250 W



tungsten halogen lamp. A water filter was introduced between the light source and the PEC cell to cut off the IR portion. The intensity of illumination was measured with a CEL suryama-pi, whose readings are directly calibrated in mWcm⁻². The intensity of illumination was varied changing the distance between the source and the cell. The power output characteristics of the cells were measured by connecting the resistance box and an ammeter in series and the voltage output was measured across the load resistance. The photocurrent, dark current and output voltage were measured with a HIL digital multimeter.

The CIAS photoelectrodes were dipped in the electrolyte and allowed to attain equilibrium under dark conditions for about 10 minutes. The dark current and voltage values were noted. The cells were then illuminated by the light source and the current and voltage were measured for each setting of the resistance box. The photocurrent and photovoltage were calculated as the difference between the current under illumination and the dark current, and voltage under illumination and dark voltage respectively. The intensity of the light falling on the films deposited at different duty cycles was kept constant at 60 mW cm⁻².

Illumination of the interface with light of suitable wavelength that shows a photovoltaic effect is an important technique to determine the properties of semiconductor/electrolyte interfaces. The PEC cells using these films exhibited very low photocurrent and photovoltage. Amongst the films deposited at different duty cycle, films deposited at 50 % duty cycle exhibited maximum photocurrent and photovoltage.

tion of grain boundaries due to prolonged photoetching [17].

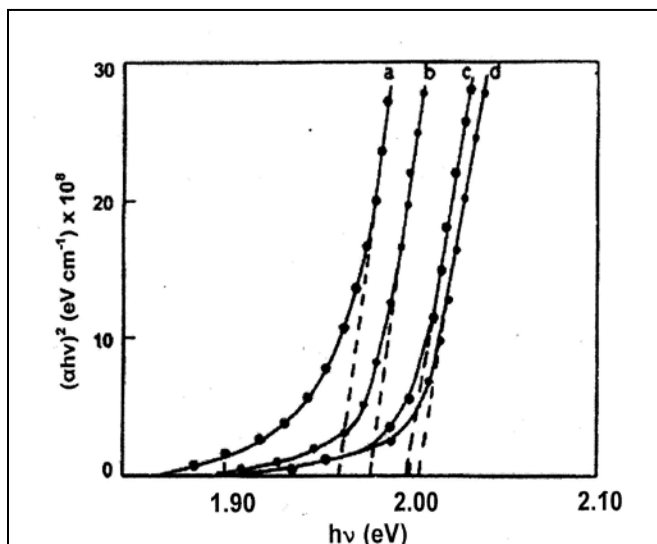


Fig.3 - Tauc's plot of CIAS films deposited at different duty cycles (a) 6 % (b) 15 % (c) 33 % (d) 50 %

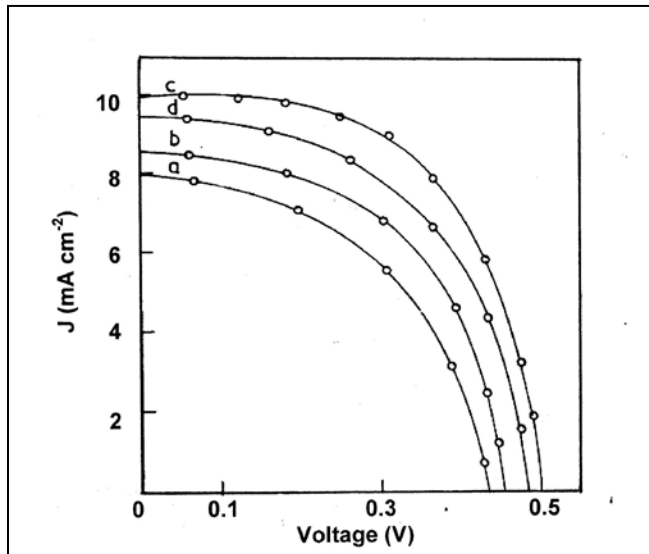


Fig.4 - Load characteristics of CIAS films deposited at 50 % duty cycle and post heated at different temperatures (a) 450°C (b) 475°C (c) 500°C (d) 525°C

Hence, further studies were made on the films deposited at 50 % duty cycle. The as deposited films exhibited low photoactivity, amongst the films, those deposited at 50 % duty cycles exhibited maximum photo output. In order to increase the photo output, the films deposited at 50 % duty cycle were post heated in argon atmosphere at different temperatures in the range of 450 - 525°C for 15 min. Fig.4 shows the load characteristics of the post heat treated films. From the figure, it is observed that the PEC output parameters, viz., open circuit voltage and short circuit current were found to increase for the electrodes heat-treated upto a temperature of 525°C. Photoelectrodes heat-treated at temperatures greater than this value exhibited lower open circuit voltage and short circuit current due to the reduction in thickness of the films as well as the slight change in stoichiometry. The photovoltaic parameters are shown in Table II. For a film deposited at 50 % duty cycle and post heat treated at 500°C, an open circuit voltage of 0.50 V and a short circuit current density of 10.0 mA cm^{-2} were observed at 60 mW cm^{-2} illumination. Both V_{oc} and J_{sc} increased with increase of intensity. Beyond 80 mW cm^{-2} illumination, V_{oc} was found to saturate as is commonly observed in the case of photovoltaic cells and PEC cells, J_{sc} is found to linearly increase with intensity of illumination. A plot of $\ln J_{sc}$ vs V_{oc} yielded a straight line. Extrapolation of the line to the y-axis yields a J_0 value of $1.15 \times 10^{-7} \text{ A cm}^{-2}$, the ideality factor (n) was calculated from the slope of the straight line and it was found to be 2.05.

Photoetching was done by shorting the photoelectrodes and the graphite counter electrode under an illumination of 100 mW cm^{-2} in 1 : 100 HNO_3 for different durations in the range 0 - 100s. Both photocurrent and photovoltage are found to increase up to 80s photoetch, beyond which they begin to decrease. This is illustrated in Fig.5 for the photoelectrode deposited at 50 % duty cycle. The decrease of the photocurrent and Photo voltage after 80s photoetch may be attributed to separa-

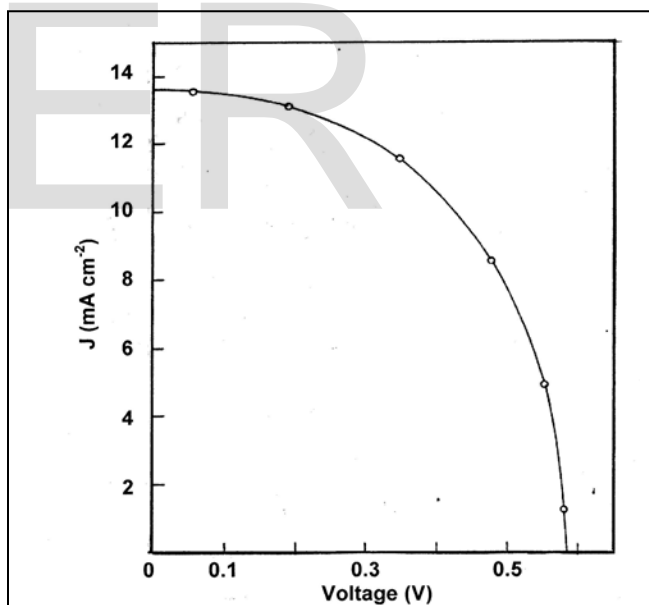


Fig.5 - Load characteristics of CIAS films deposited at 50 % duty cycle and post heated at 500°C after photoetching for 80s.

The power output characteristics (Fig.5) after 80s photoetching indicates a V_{oc} of 0.60V, J_{sc} of 7.53 mA cm^{-2} , ff of 0.53 and η of 3.98 %, for 60 mW cm^{-2} illumination. The photovoltaic parameters of the electrodes with and without photoetching are shown in Table.4.

Photoetching process successfully decreases the density of recombination centers by etching out surface steps and imperfections. This leads to improvement in photocurrent (the

maximum observed increase in photocurrent was by more than 3 times and hence conversion efficiencies. It was found that surface steps, inhomogenities and defects are etched/ removed as a result of photoetching. The photoetching process has been generally found to result in a slight increase in the photovoltage (open circuit voltage). This has been found to be a consequence of the change in flat band potential.

Photoetching is apparently one of the most promising surface treatment process for enhancement of conversion efficiency through suppression of recombinations. The fill factor (FF) is another important PEC parameter which manifests the solar-toelectrical energy conversion efficiency of the cell. It reflects the ability of photogenerated current to perform work through an external load and is therefore very sensitive to the kinetics of current flow through the semiconductor/ electrolyte interface. It has been found that in addition to photocurrent, the fill factor gets enhanced, but to a lesser degree as a result of photoetching. The dominant reason for this is thought to be a decrease in recombination velocity of minority carriers. The improvement in the fill factor indicates the fact that the semiconductor/ electrolyte interface behaves closer to the ideal case after photoetching, i.e., the dark saturation current decreases (shunt resistance increases), (series resistance decreases). A side result of photoetching is a decrease in reflectivity and hence an increase in absorptivity of light leading to a better conversion efficiency. It is thought that the decrease in reflectivity occurs due to the formation of microetch pits on the electrodes and hence a roughening of the surface steps upon photoetching. Similar behaviour was observed in WSe₂ photoelectrodes [18].

Table – II
Photovoltaic parameters of CuIn_{0.6}Al_{0.4}Se₂ films deposited at 50 % duty cycle and post heat treated at different temperatures (Intensity – 60 mW cm⁻²)

Heat treatment Temp (°C)	Voc (mV)	Jsc (mA cm ⁻²)	ff	η (%)	Rs (Ω)	Rsh (k Ω)
450	420	8.00	0.55	3.08	40	1.75
475	435	8.50	0.58	3.57	37	1.85
500	500	10.00	0.65	5.42	31	1.90
525	485	9.50	0.60	4.61	28	2.00
500	590	13.70	0.65	8.75	14	2.50

(After photoetch)

4 CONCLUSIONS

Single phase nanocrystalline CuIn_{0.6}Al_{0.4}Se₂ films could be deposited by the pulse electrodeposition technique. The band gap of the films can be adjusted from 1.97 eV to 2.07 eV with increase of duty cycle. Photoelectrochemical solar cells exhibiting 8.75 % efficiency can be fabricated with the films.

REFERENCES

- [1] M.A. Contreras, K. Ramanathan, J. AbuShama, F. Hasoon, D.L. Young, B. Egaas, R.Noufi, "Diode characteristics in the state of the art ZnO/CdS/CuIn_{1-x}GaxSe₂ solar cells", Prog. Photovolt. 13, No.3 (2005) 209 - 216.
- [2] M.W. Haimbodi, E. Gourmelon, P.D. Paulson, R.W. Birkmire, W.N. Shafarman, 28th IEEE Photovoltaic Specialists Conference, September 2000, p. 454, Alaska, U.S.A.
- [3] S. Marsillac, P.D. Paulson, M.W. Haimbodi, R.W. Birkmire, W.N. Shafarman, "High efficiency solar cells based on ChInAlSe₂ thin films", Appl.Phys. Lett. 81, No.7 (2002) 1350 - 1354.
- [4] Y.B.K. Reddy, V.S. Raja, B. Sreedhar, "Growth and characterization of CuInAlSe₂ thin films by co-evaporation", J. Phys. D: Appl. Phys. 39, No.24 (2006) 5124 - 5132.
- [5] B. Kavitha, M. Dhanam, " In and Al composition of nano-CuInAlSe₂ films from XRD and transmittance", Mater. Sci. Eng., B 140, No.1-2 (2007) 59 - 63.
- [6] B. Munir, R.A. Wibowo, E.S. Lee, K.H. Kim, "One step deposition of CuInAlSe₂ films by magnetron sputtering", J. Ceram Process. Res. 8, No.4 (2007) 252 - 255.
- [7] J.Lopez-Garcia, C.Maffiotte, C.Guillen, "Wide band gap CuInAlSe₂ films grown on conducting oxide", Solar Energy Materials & Solar Cells 94, No.7 (2010) 1263-1269.
- [8] F. Liu, C. Huang, Y. Lai, Z. Zhang, J. Li, Y. Liu, "Preparation of CuInGaSe₂ films by pulse electrodeposition", J. Alloys Compd. 509, No.8 (2011) L129-L133.
- [9] S. Mandati, B.V. Sarada, S.R. Dey, S.V. Joshi, " Pulse electrodeposition of CuInSe₂ films with morphology for solar cells", J. Electrochem. Soc. 160, No.4 (2013) D173-D177.
- [10] S. Mandati, B.V. Sarada, S.R. Dey, S.V. Joshi, : Improved photoelectrochemical performance of CuInGaSe₂ thin films prepared by pulse electrodeposition", J.Renew. Sustain. Energy 5, No.3 (2013) 031602.
- [11] S. Mandati, B.V. Sarada, S.R. Dey, S.V. Joshi, " CuInGaSe₂ films for photovoltaic solar cell applications by two stage pulse current electrodeposition", Mater. Lett. 118 (2014) 158- 160.
- [12] Y.Bharat Reddy, V.Sundara Raja, " Preparation and characterization of CuIn_{0.3}Al_{0.7}Se₂ films for tandem solar cells", Solar Energy Materials & Solar Cells 90 , No.11(2006) 1656-1665.
- [13] M.C.Santhosh Kumar, B.Pradeep, "Formation and properties of AgInSe₂ films by co-evaporation", Vacuum, 72, No.4 (2004) 369 - 378.
- [14] S. Endo, Y. Nagahori, S. Nomura, " Preparation of CuInSe₂ films by pulse electrodeposition", Jpn. J. Appl. Phys. 85, No.9A (1996) L1101 - L1103.
- [15] H. Karaagac, M. Kaleli, M. Parlak, "Characterization of Ag-Ga_{0.5}In_{0.5}Se₂ thin films deposited by electron beam evaporation", J. Phys. D Appl. Phys. 42, No.16 (2009) 165413
- [16] F. Smaili, M. Kanzari, B. Rezig, "Characterization of CuInAlSe₂ films prepared by thermal evaporation", Materials Science and Engineering C 28, No.5-6, (2008) 954-958.
- [17] J.P.Mangalharaj, R.Thangaraj, O.P.Agnihotri. " Photoelectrochemical conversion using spray pyrolysed CdSe films",Bull. Mater.Sci; 10, No.1 (1988) 333 - 340.
- [18] G. Prasad and O.N. Srivastava, " The high efficient WSe₂ photoelectrochemical solar cells", J. Phys. D., 21, No.6, (1988) 1028 - 1030.